

Supporting information

Uselman, Barto, Jacobs and Bearer

Fig S1: Diagram of a hypothesis of how acute fear may resolve or persist.

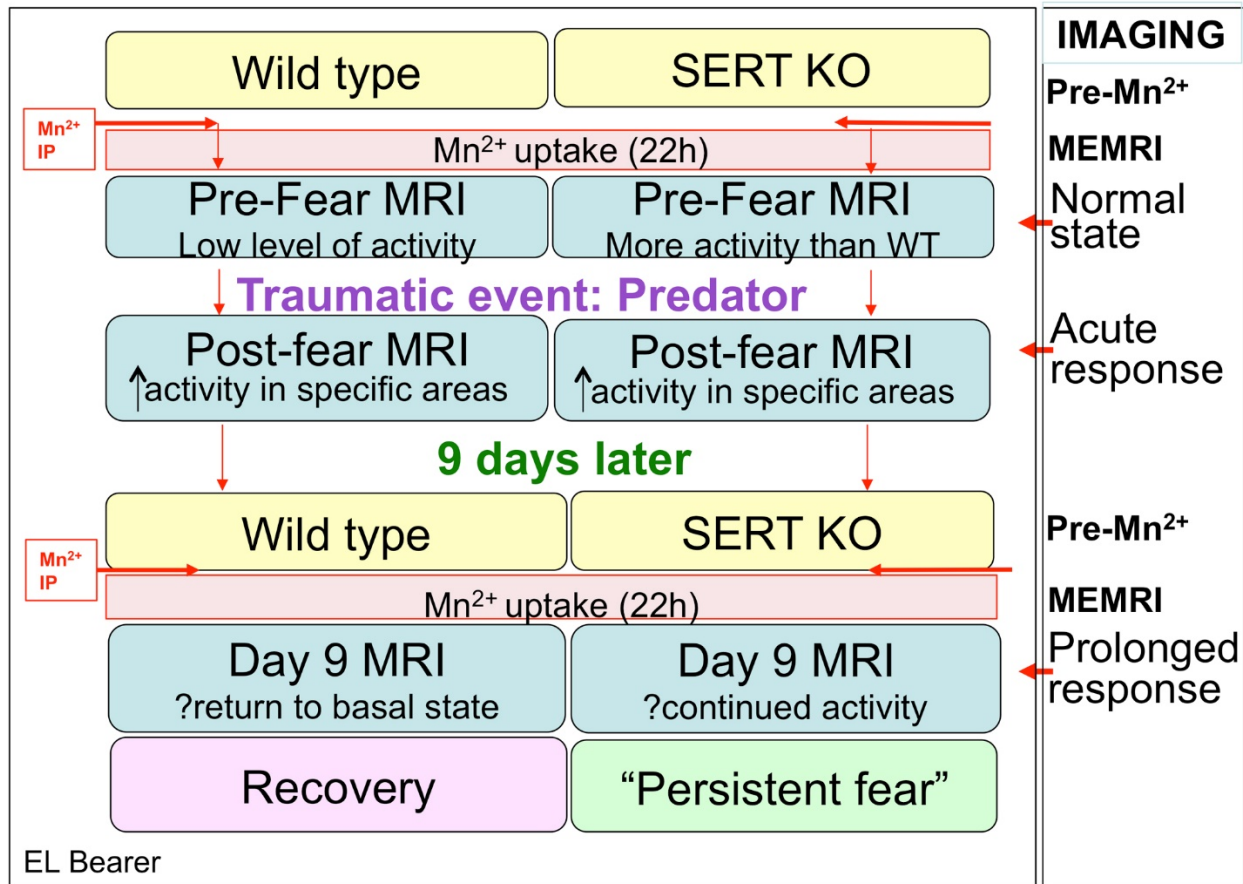


Fig S1: Diagram of a hypothesis of how acute fear may resolve or persist. Wild type (WT) and SERT-KO mice differ in their ability to recover to baseline activity after a traumatic event (predator odor, PO). While WT recover, SERT-KO remain in a fearful state. We hypothesize that this behavior reflects differences in neural activity in the brain, which we test directly with MEMRI brain-wide imaging. Horizontal red arrows indicate Mn²⁺ IP injections, and vertical arrows in red boxes indicate Mn²⁺ uptake into active neurons in naturally behaving, freely moving mice. Blue boxes represent three imaging sessions after Mn²⁺ injection: Pre-Fear, Post-Fear and 9 days later (Day 9). Only one fear exposure is performed. We predicted that WT, with low neural activity prior to predator stress, responds to fear with increased activity, which resolves to Pre-Fear levels by 9 days afterwards. In contrast, SERT-KO has more neural activity prior to traumatic event, which increases in response to trauma. Unlike WT, activity in SERT-KO will not resolve at 9 days but continue and may evolve to new regions. This continued activity will manifest as defensive behavior in SERT-KO. In WT, some residual neural activity post-trauma may be present but at levels too low to produce an observable behavioral correlate.

Fig.S2: Examples of individual images after skull-stripping (A) and averaged images of the datasets after alignment (B)

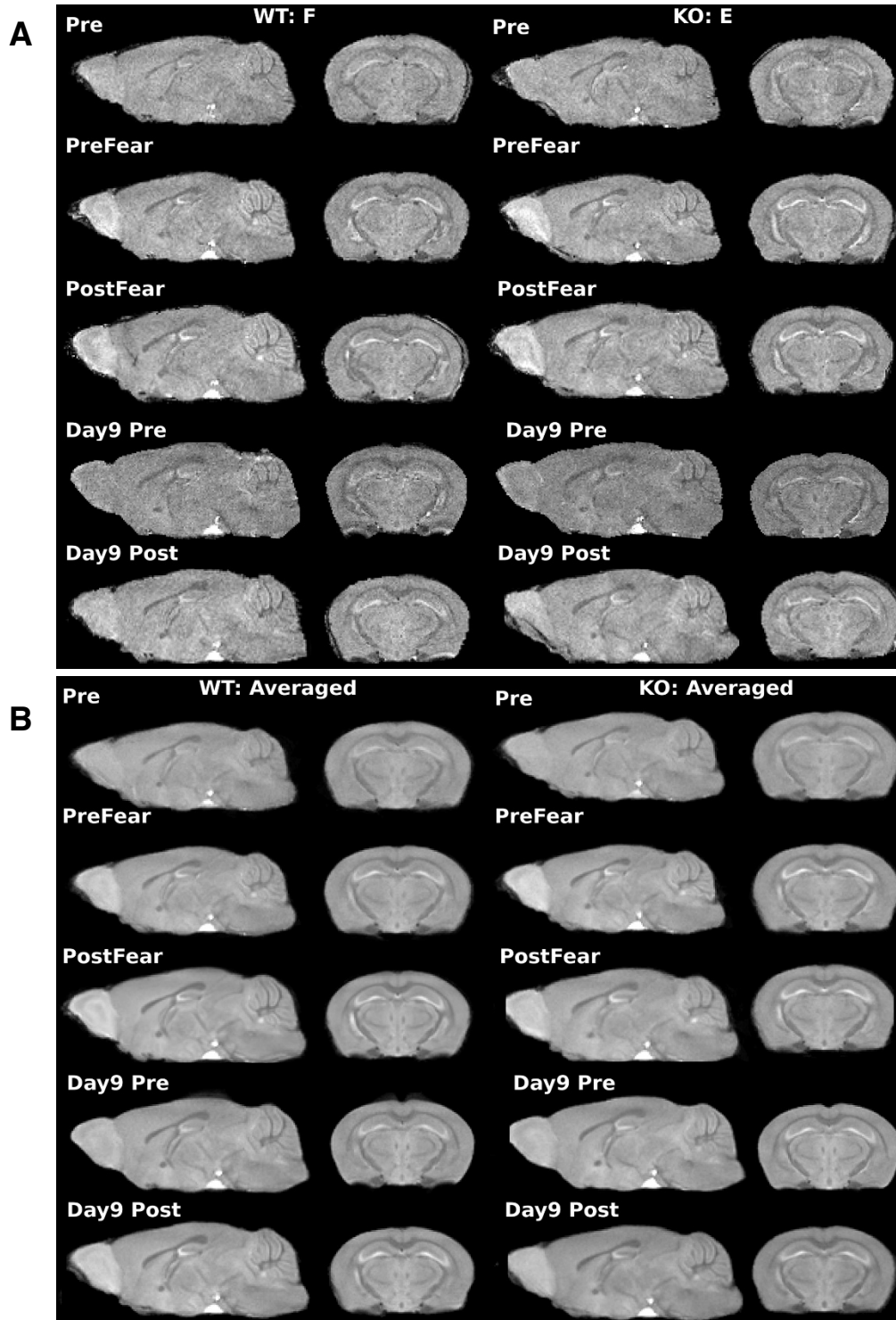


Fig.S2: Examples of individual images after skull-stripping (A) and averaged images of the datasets after alignment (B). NOTE: Averaging the four Post-Fear images (B) does not increase signal over single image (A)

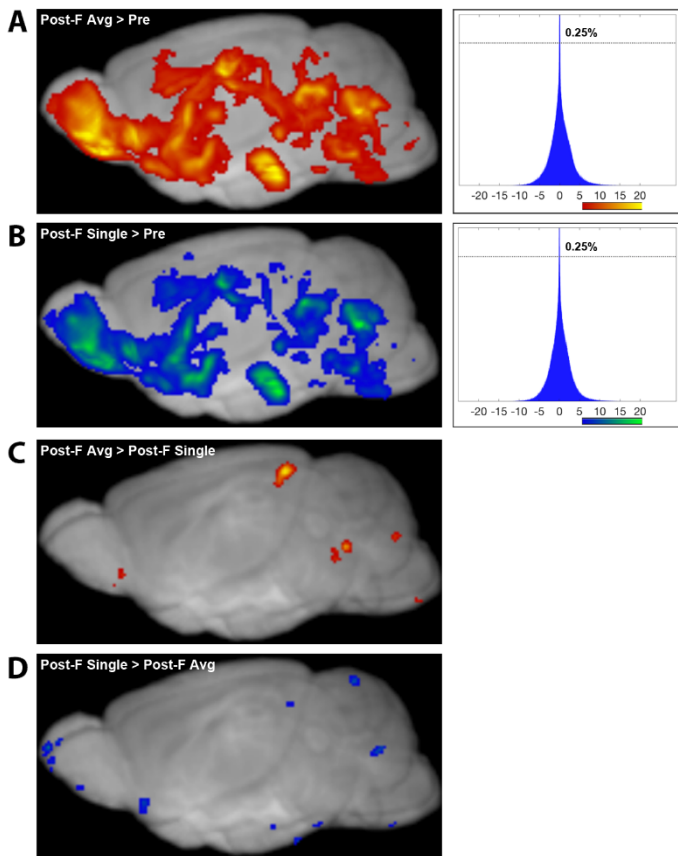


Fig. S3: Averaging four Post-Fear images results in only very minor differences in SPM.

Rationale and Method: To determine if averaging the series of four Post-Fear images improved enhanced statistically significant signal, we performed additional SPM comparisons between averages of 4 Post-Fear images and the fourth single Post-Fear image from that 4-image dataset (n=12). Two sets of pairwise t-tests were compared: (1) Averaged Post-Fear images (Post-F Avg>Pre) versus single Post-Fear images (Post-F 4>Pre), each to pre-injection images (**Fig. S3, A & B**); and (2) Single and averaged Post-Fear images compared in SPM to each other (**Fig. S3, C & D**). As before, we required a minimum voxel cluster size of 128 for significance at $p<0.0001$ uncorrected ($T=5.4$), the same statistic used for the other comparisons throughout this paper.

T-distribution histograms of SPM maps (**Fig. S3A and B**, right panels) confirmed the impression that averaging did not enhance sensitivity. If there were an increase in effect size and a decrease in variance produced by the averaging, we would see differences in the t-value histograms. Instead, 0.25% of the voxels in both single and averaged images reached the peak of the histogram, the variance was between -10 and +10 in both, and the ranges are approximately similar, -20 to +20.

Direct comparison of the single images to the averaged images detected only a few regions (**Fig. S3, C & D**). These regions likely represent those activated uniquely during the time frame of the fourth image and lost in the averaging procedure.

Figure Legend:

Fig. S3: Averaging four Post-Fear images results in only minor differences in SPM.

A-B) Snapshots of MRIcron 3D renderings and t-value histograms after paired t-tests in SPM contrasting Post-Fear images with pre-injection images. Results are overlaid on a gray scale template (left) and corresponding histogram of t-value distribution (right). **A)** Averaged Post-Fear images relative to pre-injection images (left) (red-yellow gradient according to t-value, see horizontal axis of the histogram for color-code). Corresponding t-value distribution is shown as a histogram (right). The line at the top of the graph labeled 0.25% indicates the percent of voxels at the mode. **B)** Single Post-Fear images relative to pre-injection images (left) (blue-green gradient according to t-value, see horizontal axis of the histogram for color-code). Corresponding t-value distribution is shown as a histogram (right) ($p<0.0001$, $T=5.4$).

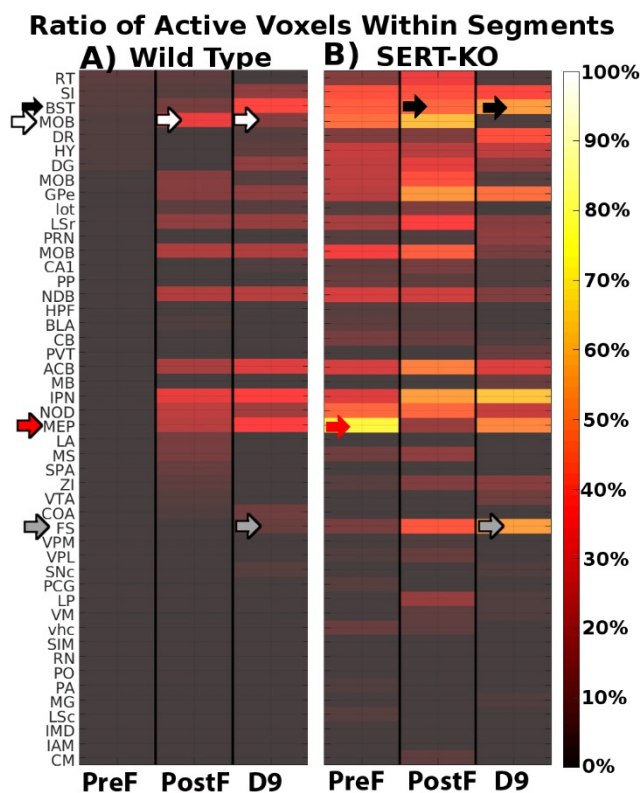
C-D) Comparison between averaged Post-Fear images and single Post-Fear images. **C)** Averaged images with signal greater than single images (color code as in A). **D)** Averaged images with signal less than single images (color code as in B) ($p<0.0001$, $T=5.4$).

Conclusion: Only minor differences are found in SPM analyses between averaged Post-Fear images and a single image from the same dataset and the pre-injection image and between each other. Although these differences are small, they could be meaningful about progression of activity over the 2 hours immediately following a single fear exposure for future study. Hence, averaging is not responsible for the large amount of increased signal from Pre- to Post-Fear.

more stereotypical and uniform across individuals than WT, possibly a consequence of the disrupted neuromodulatory serotonergic system.

All 87 segments are shown. The order of segments is alphabetical, as in Table 1, which provides an alphabetized list of abbreviations.

Fig. S5: A heat map showing how the ratio of active voxels compared to total voxels within each segment evolves over time. In the heat map, segments are ranked according to the WT Pre-Fear analysis, from high (top) to low. (See Supplemental Table S1 for abbreviations).



A) WT; B) SERT-KO. Total number of voxels in each segment were determined from the *InVivo* Atlas, and the number of active voxels within each segment obtained from segmented SPMs at each time point ($p < 0.0001$ *uncorr.* $T = 5.4$). The heat map color code is indicated on the right. Calculations were performed in a custom MATLAB script (see Material and Methods, main text).

The heat map shows little activity in the WT Pre-Fear (first column), with a larger number of segments in the SERT-KO both at Pre-Fear (fourth column) and post-Fear (fifth column). One segment stands out in the Pre-Fear data in SERT-KO: the median pre-optic nucleus (MEP) (see **Table 1** for abbreviations) (red arrow pointing to the yellow cell in the SERT-KO RS column). The MEP is a small nucleus in the hypothalamus with both inhibitory and excitatory connections throughout the brain in mouse and human. The heat map also demonstrates many other differences in specific regions across time points. For example, Post-Fear in both genotypes displays activity in numerous regions, with many more regions containing activity in SERT-KO than WT. Many of the brightest regions in the heat map in SERT-KO Post-Fear also have activity in WT but to a lesser extent. These areas included sensory systems, such as the main olfactory bulb, and association areas in the striatum, such as the diagonal band (NDB), interpeduncular nucleus (IPN) and globus pallidus (GP). One segment, the fundus of striatum (FS, gray arrow),

displayed 41% active voxels in the SERT-KO. Of the 48 segments shown here, 31 displayed >5% increased volume of active voxels in the Post-Fear image for SERT-KO.

At Day 9 (D9) the WT has sustained, increased and decreased active voxels compared to Post-Fear. WT sustains some in the lateral septum, nucleus accumbens, and interpeduncular nucleus, and has 2-3 regions with increased activity such as the bed nuclei of the stria terminalis and substantia innominata. WT also displays decreases in the main olfactory bulb (MOB) and subparafascicular area (SPA), despite baseline exploratory non-defensive behavior in the light-dark box. SERT-KO at Day 9 has more active voxels than WT in the bed nuclei of the stria terminalis (BST) (black arrows) and substantia innominata (SI). SERT-KO accumulation in the main olfactory bulb (MOB, white arrows) is even further decreased than WT at D9 (third and sixth columns). SERT KO also show some increases at D9 over Post-Fear in the lateral amygdala (LA), bed nuclei of the stria terminalis (BST) and interpeduncular nucleus (IPN).

MEMRI detected increased activity compared to pre-Fear even though exploratory behavior had reverted to baseline exploratory behavior in WT, suggesting a neural signature for the memory of fear that is not strong enough to produce an observable behavioral effect. Indeed, it may be naive to believe that mouse brain activity always displays as a measurable behavior. Different ordering of these activity graphs reveals different information.

Fig. S6. Between group comparison of WT and SERT-KO across all time points.

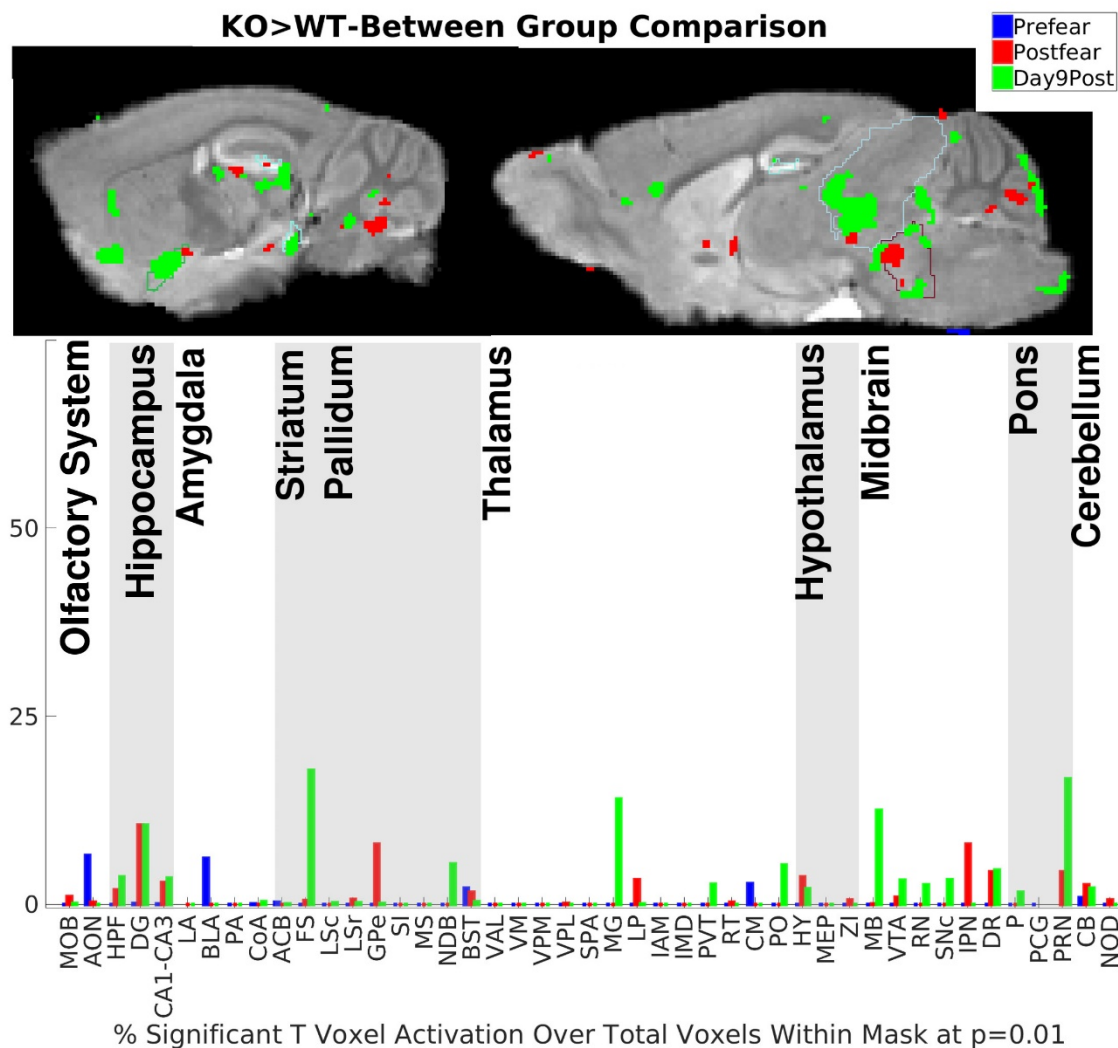


Fig. S6. Between group comparisons of WT and SERT-KO across all time points.

The SPM images from a two-sample t-test (top) identify regions where SERT-KO intensity increase is significantly greater than that of WT ($p < 0.01$ uncorr., $T=2.7$). Column graphs (bottom) show segments where the volume of significantly enhanced voxels is greater in SERT-KO than WT. Pre-Fear (blue); Post-Fear (red) and Day 9 pre (yellow) to Day 9 post $Mn^{2+}IP$ (green). At Day 9, a greater volume of activity in SERT-KO appears in FS, NDB, MG, MB and PRN compared to WT. Our ROI analysis (**Fig. 9B**) demonstrated that the degree of difference in these areas at Day 9 was statistically significant as well. This analysis demonstrates that the major differences between genotypes are at Day 9 when behavior is also divergent.

References for Supporting Information

1. Price JL, Drevets WC. Neurocircuitry of mood disorders. *Neuropsychopharmacology*. 2010;35(1):192.
2. Adolphs R. The biology of fear. *Current Biology*. 2013;23(2):R79-R93.
3. Lang PJ, Davis M, Öhman A. Fear and anxiety: animal models and human cognitive psychophysiology. *Journal of affective disorders*. 2000;61(3):137-59.
4. Davis M, Walker DL, Miles L, Grillon C. Phasic vs sustained fear in rats and humans: role of the extended amygdala in fear vs anxiety. *Neuropsychopharmacology*. 2010;35(1):105.
5. VanElzaker MB, Dahlgren MK, Davis FC, Dubois S, Shin LM. From Pavlov to PTSD: the extinction of conditioned fear in rodents, humans, and anxiety disorders. *Neurobiology of learning and memory*. 2014;113:3-18.
6. Tovote P, Fadok JP, Lüthi A. Neuronal circuits for fear and anxiety. *Nature Reviews Neuroscience*. 2015 05/20/online;16:317.
7. Silva BA, Gross CT, Gräff J. The neural circuits of innate fear: detection, integration, action, and memorization. *Learning & memory (Cold Spring Harbor, NY)*. 2016;23(10):544-55. PubMed PMID: 27634145.